

Cypermethrin Cause Allergic Inflammatory Response in Rat Lung

Cristina GR¹, Marcela RLE², Lourdes AMM³, Javier VJ¹, Humberto MOM⁴, Carolina VMC¹ and Consolación MSM^{1*}

¹Departamento de Morfología, Universidad Autónoma de Aguascalientes, Aguascalientes, México

²Departamento de Ingeniería Bioquímica, Universidad Autónoma de Aguascalientes, Aguascalientes, México

³Departamento de Investigación y posgrado en alimentos, Universidad de Sonora, Boulevard Luis Encinas J, México

⁴Departamento de Química, Universidad Autónoma de Aguascalientes, México

*Corresponding author:

Martínez-Saldaña Ma. Consolación,
Departamento de Morfología, Universidad,
Universidad Autónoma de Aguascalientes, Av.
Universidad 940, CP 20131, Aguascalientes, Ags.,
México

Received: 19 Nov 2023

Accepted: 11 Dec 2023

Published: 18 Dec 2023

J Short Name: AJSCCR

Copyright:

©2023 Consolación MSM, This is an open access article distributed under the terms of the Creative Commons Attribution License, which permits unrestricted use, distribution, and build upon your work non-commercially.

Keywords:

Cypermethrin; Inhaled toxicity; Inflammatory reaction; IL-4; IL-5; IL-13; IgE

Citation:

Consolación MSM. Cypermethrin Cause Allergic Inflammatory Response in Rat Lung. *Ame J Surg Clin Case Rep.* 2023; 7(5): 1-9

1. Abstract

Cypermethrin is a type 2 photosensitive liposoluble pyrethroid for agricultural and domestic use, has a half-life in the ambient air for days, its metabolism in human liver generates a cyan group (CN), an alcohol fraction (dimethylcyclopropanecarboxylic acid) (DCCA), and 3-acid phenoxybenzoic acid (3-PBA) with reactive oxygen species (ROS) properties, there are scarce studies when is inhaled. The objective of this work was to evaluate the structural changes and activation of allergic inflammatory response in lower airway components and alveoli induced by inhaled exposure to low doses of cypermethrin. Rats were exposed during 7, 14 and 21 days by inhalation, then were analyzed the serum levels of IgE by ELISA, performed H&E stain on lung tissue for analyze the structural changes, through immunofluorescence were detected positive cells to IL-4, IL-5 and IL-13, finally by qPCR was quantified mRNA for IL-4, our results shows that cypermethrin induce a local and systemic allergic inflammatory reaction in rats, specifically in lungs, induce the production and secretion of products of Th2 cells (IL-4, IL-5, IL-13), eosinophils and, high serum levels of IgE, demonstrating like this, the cytotoxic effect of cypermethrin at 7 and 14 days exposition.

2. Introduction

Cypermethrin is a type 2 photosensitive liposoluble pyrethroid for agricultural and domestic use, has a half-life in the ambient air for days [1, 4], is widely used in Mexico for control of domestic and field pests [9]. Due to its fat-solubility, it is easily absorbed dermally, gastrointestinal and inhaled. Respiratory exposure requires that the particle size of the respirable fraction be 0.5 to 5

µm, to reach the lower airway and alveoli [7]. After systemic absorption, cypermethrin is hydrolyzed in the liver by human carboxylesterase 1 (hCE-1), generating a cyan group (CN), an alcohol fraction (dimethylcyclopropanecarboxylic acid) (DCCA), and 3-acid phenoxybenzoic acid (3-PBA); the cyan and acid fractions form conjugates with several compounds for their elimination, if the cyan group does not conjugate, then it forms the thiocyanate anion (-SCN) that increases oxidative stress, a part of the alcohol fraction is conjugated and removed by urine and feces, while the other part, is oxidized in carbon 4 of the phenoxybenzoic ring to form the compound 4-hydroxyphenoxy benzoic acid (4OH3PBA), the latter compound is oxidized by several isoforms of cytochrome P450 (2E1) in human and in rat generating reactive oxygen species (ROS) [11]. In humans, its half-life is 10 hours [11, 16]. Toxicity to exposure to this compound has been reported, manifested as an allergic inflammatory response in lung tissue [3]. Allergy-like inflammation in mucous membranes, is induced by the disruption of epithelial barriers by allergens and contaminants through two mechanisms [8], a) by the secretion of cytokines derived from the epithelium that activate innate lymphoid cells from group 2 (ILC2) (IL-5, IL-9 and IL-13) and to the dendritic cells (DC) of the lamina propria; b) DC endocytoses the allergens in the lung, they are activated and migrated to the lymph nodes of the bronchial-associated lymphoid tissue (BALT) where they present the antigen to TH2 lymphocyte and activate it, the TH2 cell activation process results in the production and secretion of cytokines IL-4, IL-5, IL-9 and IL-13 [14, 18]. IL-4, in turn, promotes the production of IgE responsible for activating mast cells, a cell that releases inflammatory mediators (histamine, leukotriene C4 (LTC4) and

IL-8) [6], and induce smooth muscle contraction, increase in vascular permeability and recruitment of inflammatory cells. IL-5 is related to the proliferation and differentiation of eosinophils, IL-9 facilitates proliferation of TCD4 + cells and mast cell activation, IL-13 modulates the response of B lymphocytes and promotes the production of IgE [14, 23], responsible for airway hyperreactivity (AHR) as occurs in asthma and allergic rhinitis [15], although the neurotoxicity of cypermethrin is well established [14], damage to other organs has been less studied; For volatile environmental allergens and pollutants, the respiratory system is the main route of exposure, producing adverse health effects [10]. The objective of this work was to evaluate the structural changes and activation of allergic inflammatory response in components of the lower airway and alveoli induced by inhaled exposure to low doses of cypermethrin.

3. Methodology

3.1. Inhaled Model

A Wistar rat model of inhaled full body exposure was used, described by Wong (2016), a camera was designed where the rats group lived during the course of the experiment. The volume of air during the nebulization of cypermethrin was 54 liters with an outlet for flow of 2.5 cm. Cypermethrin-charged particles were generated with an ultrasonic Citizen® Cun 60 nebulizer with a flow of 0.266 ml / minute, and a produced particle size of 5 µm MMAD (mean aerodynamic mass diameter). The animals were exposed for 30 minutes, once a day during the treatment, at an output speed 0.05 m.h-1.

3.2. Experimental Doses

Technical grade cypermethrin (94.3%, Química Lucava®, Guajuato, Mexico) was used, preparing a solution with an estimated concentration of 156.64 µg per m3 of air, and using 0.1% deionized water + 0.1% Tween 80 as a vehicle. The dose of cypermethrin was calculated based on the amount sprayed in 30 seconds recommended in the instructions of the commercial product Raid® Total Action (cypermethrin 1g/kg, SC Johnson and Son®, State of Mexico, Mexico).

3.3. Experimental Groups

32 adults' male rats Wistar strain, 250 g average weight, without exposure to pesticides from the gestation period, 8 animals per experimental time: 0, 7, 14 and 21 days were used. They were kept at room temperature (18°C to 26°C), under a 12-hour light / dark cycle, and Nutricubos® (Purina®, Mexico) ad libitum rodent and water supply. Its use and care were according to the technical specifications of NOM-062-ZOO-1999-2001. At the end of the experimental times, blood and lung samples were obtained, which were preserved according to the study technique until processing. The animals were sacrificed by intraperitoneal sodium pentobarbital overdose (1.5 mg/kg, Pisabental PiSA® Agropecuaria, Hidalgo, Mexico).

3.4. Clinical Hypersensitivity Evaluation

To determine the severity of clinical signs induced by exposure to cypermethrin, the adapted Li et al., [20]. Scale was used, from 0 to 5 where 0 represents no sign; 1 scratched around the nose and / or head; 2 swelling around the mucous membranes of the eyes and mouth, diarrhea, piloerection, lethargy and / or lethargy with increased respiratory rate; 3 wheezing, respiratory distress and cyanosis in mouth and tail; 4 tremor or seizures followed by physical inactivity; and 5 deaths [13].

3.5. Immunodetection of IL-4, IL-5, IL-13 Positive Cells

The intravascular perfusion technique (Prophet and Armed Forces Institute of Pathology (U.S.) 1992) was performed in 3 animals of each experimental group, consisted in applied two washes with 100 ml of a solution 0.9% saline + heparin (5000U/I) and procaine (0.2%) intracardiac via, then perfusion with 40 ml of paraformaldehyde 4 %. Subsequently, the right lung was surgically removed and preserved in paraformaldehyde (4%). The proximal third portion of the lung was processed with the histological paraffin inclusion technique (Prophet and Armed Forces Institute of Pathology (U.S.) [20]), to obtain consecutive tissue cuts of 2 µm thickness that were placed on slides treated with 3-aminopropyltriethoxy-silane (Sigma A3648). Direct double immunofluorescence for IL-5 and IL-13 was performed according to the manufacturer's standard protocol, and indirect immunofluorescence for modified IL-4 by [22]. In the double direct immunofluorescence, anti-IL-13 Alexa Fluor® 488 polyclonal antibodies (eBiosciences eBio13A) were used at a dilution of 1: 200, incubation time 60 minutes at 37°C and Anti-IL5 Alexa Fluor® 594 (R&D Systems IC605T100UG) at a dilution of 1: 200, incubation time overnight at 4°C. In indirect immunofluorescence the Rabbit Anti-IL4 polyclonal primary antibody (Abcam® ab9811) was used at 1:50 dilution and overnight incubation time at room temperature and the secondary GOAT anti rabbit Alexa Fluor® 488 (Invitrogen a11008) dilution secondary antibody 1: 200, incubation 60 minutes at 37 ° C and 60 minutes at room temperature.

From each animal, three histological sections were obtained for observation under a microscope. In each section three random fields were reviewed, using an LSM 700 Zeiss® confocal microscope. Images of each field were captured with the Blue (Zeiss®) software. To quantify the emitted fluorescence, 8-bit color depth images per channel were converted with the Fiji Open-Source image processing software package software (<http://fiji.sc>).

3.6. Histopathological Evaluation

In histological sections, 2 marking techniques were performed: Hematoxylin & Eosin (Prophet and Armed Forces Institute of Pathology (U.S.) [20]) and Erythrosin B (Erythrosin B 200964-5G, Sigma Aldrich®) [2]. A morphometric study was performed by analyzing 5 random fields (100,000 µm²) at X400 per lamella

in 3 cuts of each animal. Image capture was performed on the Axioskop® 40 optical microscope (Carl Zeiss®) with the CoolSnap Color camera and Image-Pro Plus software (Kodak® 1D Image Analysis Software). The variables studied were: Thickness of the bronchiolar epithelium (µm), number of interruptions of bronchiolar epithelium per field (20,000 µm²) and thickness of the epithelium of the alveolar septum (µm). The number of eosinophils in 6 random fields (120,000 µm²) was quantified at X400 of 3 histological sections of each animal.

3.7. Quantification of IgE by ELISA

Blood was drawn by intracardiac puncture. Serum was obtained by centrifugation at 2500 g for 10 minutes (Eppendorf®-5410 Centrifuge) and divided into two portions, one for quantification of IgE, and another for quantification of cypermethrin. Samples were kept frozen at -80°C until the time of their study. At room temperature, a serum pool was prepared per treatment time with 5 µL of each sample that was mixed in an Eppendorf tube using a Vortex - Genie 2 (Scientific industries®) for 1 minute at 10 revolutions. The IgE measurement was performed in each of the pools with the Abcam® Rat IgE ELISA Kit commercial kit (ab157736) in triplicate, according to the manufacturer’s instructions.

3.8. Isolation of Total RNA and RT-qPCR

Total RNA was isolated from 100 mg of lung of the control and experimental animals with the SV Total RNA Isolation System kit (Promega, Madison, WI, USA) following the manufacturer’s protocol. Total RNA was quantified with a Biodrop (Isogen life Science, Barcelona, España) and stored at -80°C until use. Reverse transcription was performed with 500 ng of total RNA using the GoScript Reverse Transcription System (Promega). Follow-

ing, the quantitative PCR was achieved with the Maxima SYBR Green/ROX qPCR Master Mix (2X) (K0221, Thermo Scientific, Waltham, MA, USA) in a StepOne machine (Applied Biosystems) with the next programming: 50°C for 2 min, 95°C for 3 min, 40 cycles of 95°C for 45 sec and 58°C for 45 sec. Oligonucleotides were designed to target on IL-4 and β-actin as reference control (Table 1). Relative expression levels were normalized against β-actin as an internal housekeeping gene and differences were determined using ΔΔCt relative method.

3.9. Statistical Analysis

The data obtained were performed with the single-factor ANOVA statistical tests with a posthoc study with the Tukey test when the data distribution was normal; and Kruskal-Wallis with posthoc study with Dunn’s test when the distribution of the data did not meet normality, performed in Graphpad Prism software version 5.01 Graphpad software, Inc.

4. Results

4.1. Clinical Hypersensitivity Evaluation

The animals had nasal irritation and gagging arches from the first day of exposure to cypermethrin. The signs were exacerbated on the seventh day of treatment and epistaxis, piloerection, severe scratching of ears and nose, hyaline rhinorrhea, sialorrhea, diarrhea, respiratory distress, lethargy with anorexia and adipsia were added. These signs correspond to level 3 of the Li scale for the clinical evaluation of hypersensitivity [13]. Between the seventh and tenth day there was the death of 9.4% of the animals, described in level 5 of the scale [13]. From day 11 to 15, the signs of hypersensitivity decreased to level 3; and finally, from day 15 to 21 the signs of hypersensitivity decreased to level 2 (Table 1).

Table 1: Oligonucleotides used for qPCR determination of IL-4 expression levels.

Gene	Accession Number	Oligonucleotides
IL-4		Fw:
		Rv:
β-α ₂ TV	NM_031144.3	Fw: GTCGTACCACTGGCATTGTG
		Rv: GCTGTGGTGGTGAAGCTGTA

4.2. HE and Eosinophils

4.2.1. Histopathological observations H/E: The pulmonary histological structure showed gradual damage in relation to the exposure time, the normal structure of the pulmonary parenchyma is represented by cubic epithelium, and scarce underlying connective tissue, surrounded by a layer of smooth muscle and integral alveolar septa in the control group (Figure 1Aa, b), at 7 days, epithelium suffer an oedema observed in bronchiole (arrow in Figure 1Ba), and in the socket begins the acute phase of damage or exudative, with neutrophil and macrophage infiltrate, erythrocyte congestion and edema at the expense of exudate (arrow in Figure 1Bb). At 14 days, in bronchiole there are damage manifested by exfoliation of

epithelial cells that tend to form clusters previously described as Creola bodies (Yamada, Yoshihara, and Arisaka 2004) (arrow in Figure 1Ca); and in the alveoli the proliferative phase of damage due to the thickening of the alveolar walls, glandular appearance, recruitment of neutrophils and macrophages is observed (arrow in Figure 1Cb). Finally, at 21 days, there is a transition of the proliferative phase, even with a large inflammatory infiltrate (Figure 1Da), but with a tendency to return to the normal structure (Figure 1Db).

4.2.2. Eosinophils: The quantification of eosinophils in the pulmonary stroma (Figure 3), showed a significant increase in the tissue, with a statistically significant difference with p <0.0001 between the control group with 7, 14 and 21; and of the group treated

7 days with the group treated 21 days (Figure 2d).

4.2.3. Morphometry: In addition to the histological description, epithelium thickness bronchiolar morphometry (Red arrow in Figure 1Aa) was also performed, which increased towards 7 days of exposure (Red arrow in Figure 1Ba), and then decreased at 14 and 21 days of treatment (Red arrow in Figure 1Cb, Db) (Figure 2a) ($p < 0.0001$). Alveolar septum thickness (yellow line in Figure 1Ab, Bb, Cb and Db) behaved similarly to that of the epithelium bronchiolar, increasing towards 7 and 14 days with a tendency to recovery at 21 days and presented statistically significant difference between the control group with the exposed group 7, 14 and 21 days, respectively ($p < 0.0001$) (Figure 2b). Bronchiolar Epithelial disruption did not occur in the control group, and they were presented in relation to the time of exposure, being its highest peak at 21 days ($p < 0.001$) (Figure 2c).

4.3. Detection of IL-4, IL-5 e IL-13 by Immunofluorescence

4.3.1. IL-4: The control group showed positivity in the cytoplasm of the IL-4 lung parenchyma cells. Change in the distribution of IL-4 was observed based on the time of exposure to cypermethrin. The cytoplasmic distribution of positivity changed in relation to the exposure time, displacement towards the extracellular matrix was observed in the alveolar septum and increased fluorescence intensity (Figure 4), with a significant difference between the control group and the treated groups at 7, 14 and 21 days respectively, and the group 14 days with the group 21 days ($p < 0.0001$) (Figure 4).

4.3.2. IL-5 and IL-13: They are reported in parallel by the double marking carried out. In the control group, localized positivity was observed in bronchiolar epithelial cells whose intensity increased in relation to the exposure time and persists in epithelial location, the participation of IL-5 and IL-13 in the damage phase is confirmed, based on fluorescence intensity for IL-5, we detected a difference among the control group respect to the groups exposed at 7, 14 and 21 days respectively, and 7 with 14 days and 14 with 21 days ($p < 0.0001$) (Figure 5). A significant difference in the fluorescence intensity in IL-13 among control group with 7, 14 and 21 days ($p < 0.0001$) was observed (Figure 5).

4.4. IL-4 mRNA detection by qPCR

Cypermethrin induced decreased expression of the IL-4 mRNA. Analysis of the lung tissue exposed to cypermethrin decreased the expression of the IL-4 mRNA at 14 ($*P < 0.05$) and 21 days ($**P < 0.01$) during exposure in relation to the control group, while at 7 days there is no modification regarding control (Figure 6).

4.5. IgE

An increase in concentration was observed in relation to the exposure time and a difference was observed between the control group vs 7 days ($P < 0.01$), and vs 14 and 21 days ($p < 0.001$) (Figure 7).

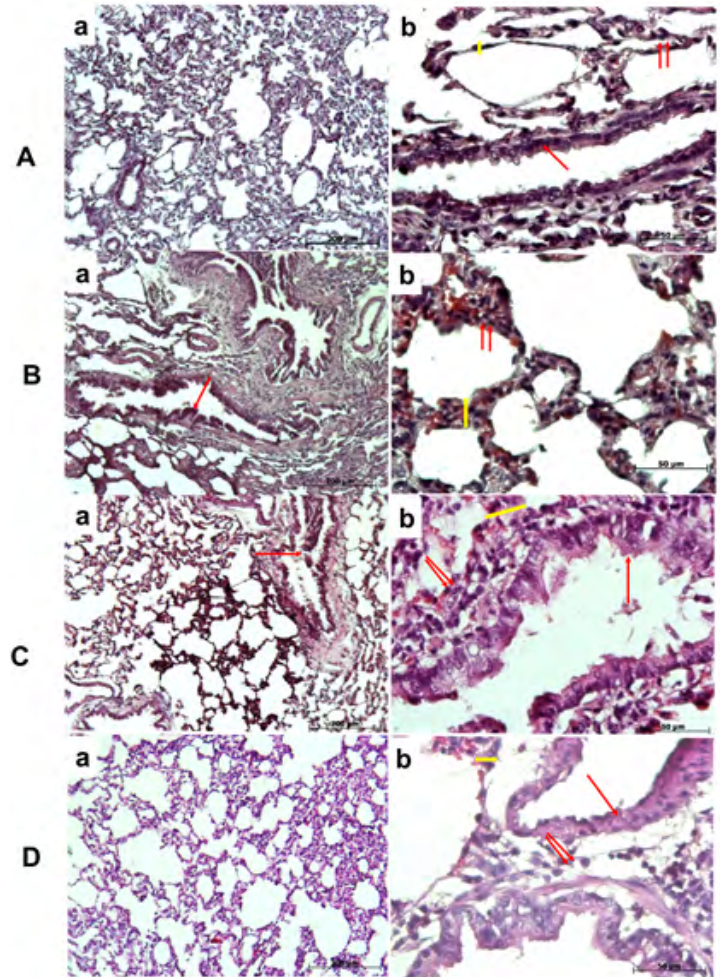


Figure 1: Morphology description of rat lung damaged by cypermethrin (H/E). Aa) Panoramic view of normal lung tissue (control), Ab) An increase of view of normal tissue, normal cylindrical epithelial cells (arrow) and slim interalveolar wall (double arrow). Ba) 7 days lung exposed to cypermethrin, panoramic view, Bb) panoramic view with hyperplasia of epithelial cells (arrow) and, Bb) Acute phase with oedema and infiltrate inflammatory cells (double arrows). Ca) Panoramic view with Creola bodies in inflamed bronchiolus. Cb) Alveoli wall with inflammatory infiltrate cells (double arrows). Da) 21 days evolution, lung tissue shows a little damage. Db) The inflammatory infiltrate in lung stroma is diminished (double arrows).

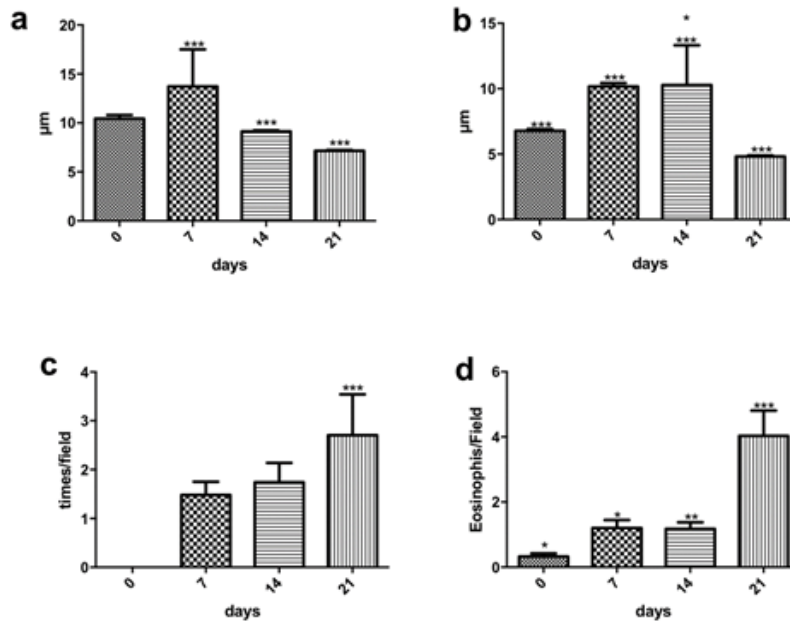


Figure 2: Morphometry for: a) Bronchiolar epithelium thickness, b) Alveolar septum thickness, c) Bronchiolar epithelial disruption, d) Eosinophils in lung tissue.

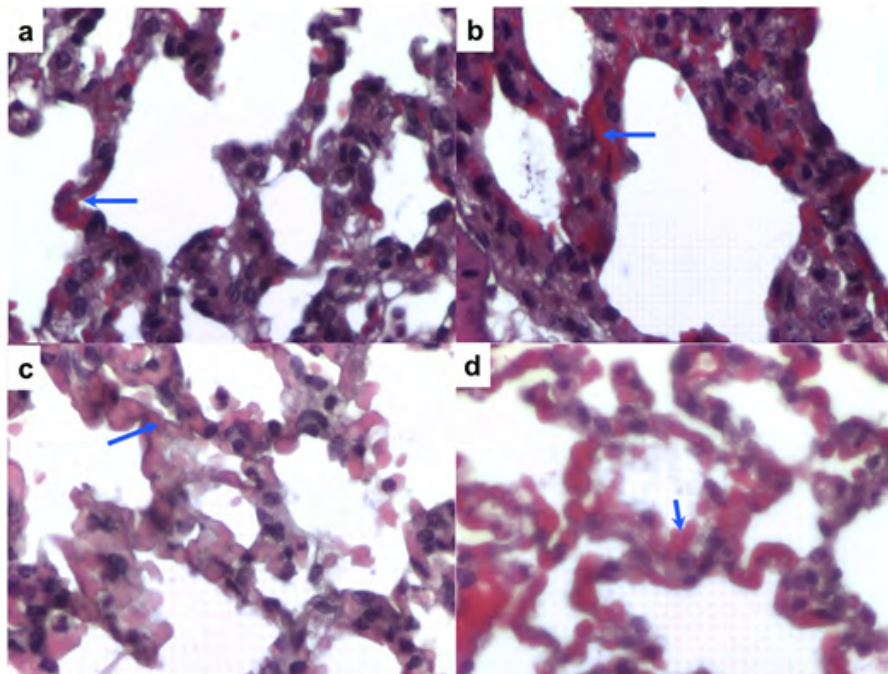


Figure 3: Eosinophils detected by Erythrosin B (blue arrow). a) normal lung (control), b) 7 days post-exposed, c) 14 days post-exposed, and d) 21 days post-exposed to cypermethrin (X400).

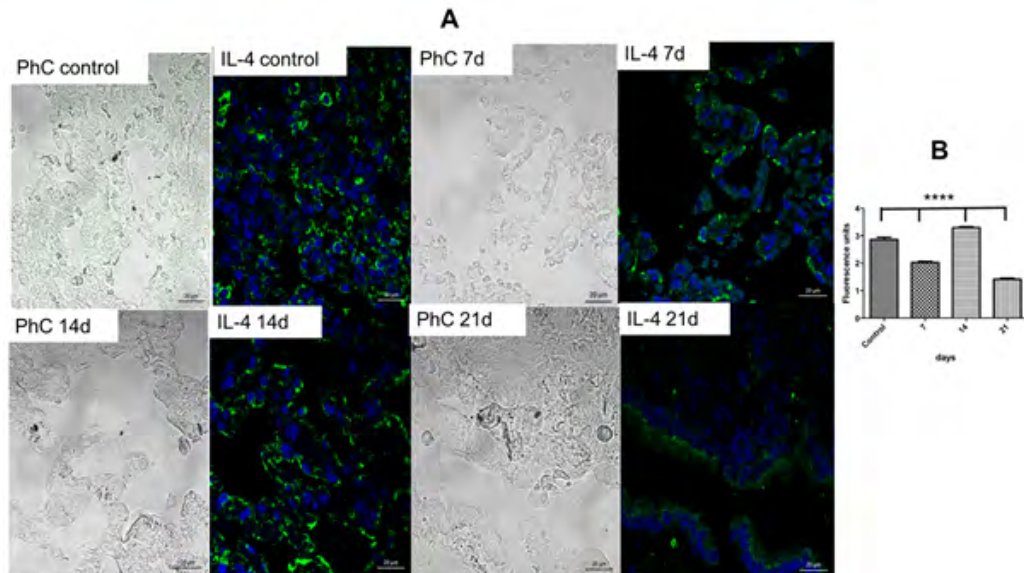


Figure 4: Immunofluorescence for IL-4, confocal microscopy images. A) PhC control= Phase Contrast control, IL-4 control= Detection of IL-4 in normal lung tissue (control), PhC 7d= Phase Contrast 7 days post-exposition to cypermethrin, IL-4 7d= Detection of IL-4 positive cells in lung tissue 7 days post-exposition, PhC 14d = Phase Contrast 14 days post-exposition, IL-4 14d = Detection of IL-4 in positive cells in lung tissue 14 days post-exposition, PhC 21d = Phase contrast 21 days post-exposition, IL-4 21d = Detection of IL-4 positive cells in lung tissue 21 days post-exposition. B) Graphics of fluorescence intensity.

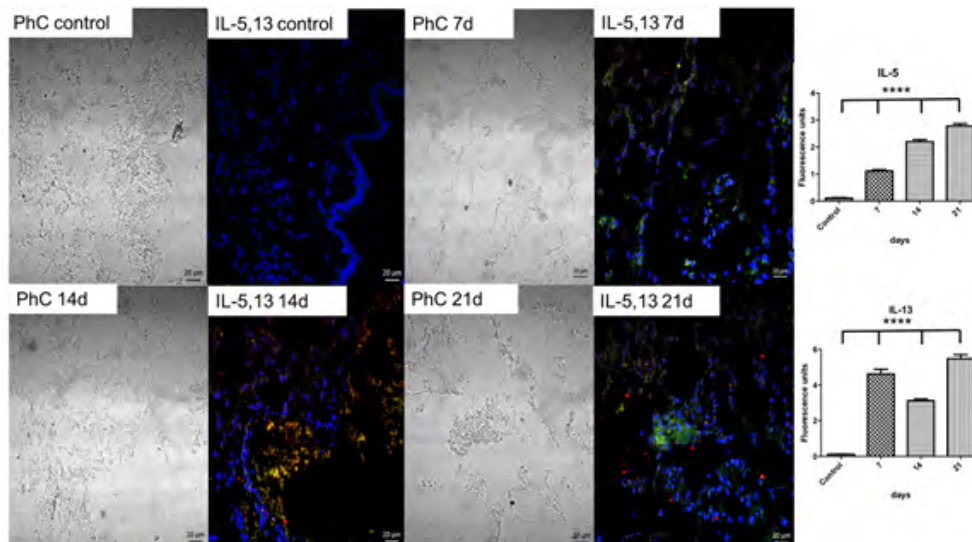


Figure 5: Immunofluorescence for IL-5 and IL-13.

Double immunodetection for IL-5 and IL-13 on rat lung tissue. PhC control = phase contrast of normal rat lung tissue; IL-5, 13 control = double Immunofluorescence for both cytokines on normal rat lung tissue; PhC 7d = Phase contrast of lung tissue during 7 days exposition to cypermethrin; IL-5, 13 7d= Double immunodetection for both cytokines, scarce positive cells for IL-5, high positive cells for IL-13 (right graphics); PhC 14d = Phase contrast of lung tissue during 14 days exposition to cypermethrin; IL-5,13 14d = Double immunodetection for IL-5,13, at 14 days exposition, middle expression of IL-5 and scarce cells positive to IL-13 (right graphics); PhC 21d = Phase contrast of lung tissue during 21 days exposition to cypermethrin; IL-5,13 14d = Double immunodetection for IL-5,13, at 21 days exposition, high expression of IL-5 and IL-13 positive cells (right graphics).

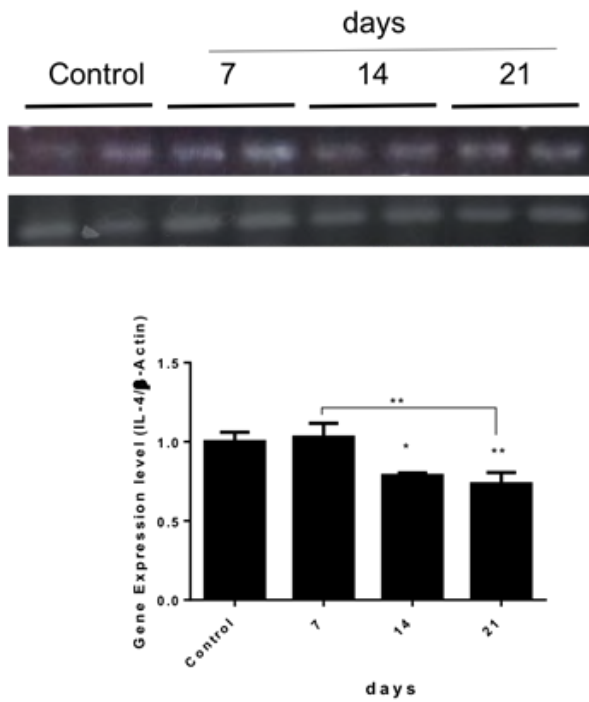


Figure 6: Cypermethrin diminish IL-4 expression in a toxicity chronic Wistar rat model.

Lung analysis shows that IL-4 had a lesser expression after exposition at 14 and 21 days to cypermethrin in relation to control, meantime, at 7 days exposition was observed some increase without different to control. Data represent a mean \pm standard deviation. * $P < 0.05$, ** $P < 0.01$.

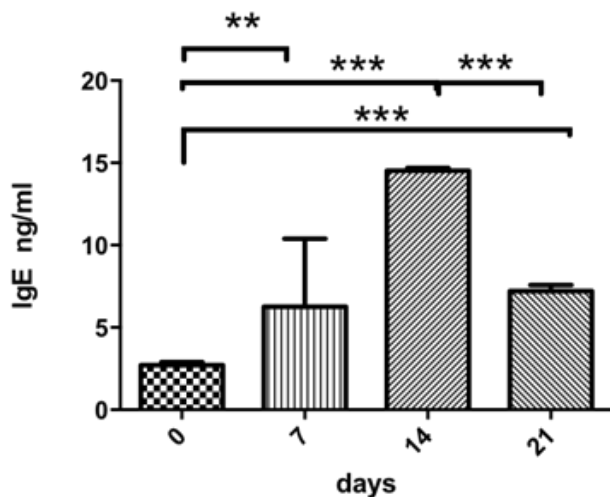


Figure 7: IgE detection by ELISA. The level of IgE antibody is raised at 7, 14 and 21 days exposition to cypermethrin, note that the high raised was at 14 days.

5. Discussion

Although there are several presentations of cypermethrin as an inhalable insecticide for domestic use, they are part of the aeroallergens and main triggers of respiratory allergies, there are few studies that review the adverse effects on the respiratory tract, so, hence the importance of studying cypermethrin inhaled to reproduce its effects before exposure and study the mechanisms related

to the pulmonary immune system. In this work it is observed that cypermethrin induces an allergy response in bronchioles and alveoli between 7 and 14 days of exposure, represented by classic clinical signs of respiratory allergy syndrome [13], damage in epithelium and bronchial stroma, local inflammatory reaction, timely increased expression of cytokines IL-5 and IL-13; but decrease in IL-4 with exception at 14 days, as well as sustained increase in serum IgE levels. Of the few studies of cypermethrin in rat Wistar, Tulinska et al., (1995), applied cypermethrin orally for 28 days to analyze its effect on splenocytes for phagocytosis, ability to respond to mitogens and activity of NK cells, found increased proliferative capacity I response to phytohemagglutinin and concanavalin A, improved NK activity, but there was no effect on phagocytic capacity, did not study the effects on the respiratory system. The near study of the effects of cypermethrin to our study, resides in what was reported by Lessenger [12], he described five cases of people accidentally intoxicated with cypermethrin, reported that people manifested immediately, shortness of breath, cough, congestion, burning eyes and itchy skin at the time of exposure, in chronicity it is described that one of the patients developed respiratory distress syndrome, as a result of this accident, it was established that cypermethrin has a toxic effect. In the rat, what can be compared with the previous signs is the arch, simulating the cough sign, increased mucus secretions by nose, scratched eyes and nose, which allows us to say that the rat has a burning sensation that and causes that behavior.

The respiratory epithelium is a structural barrier that constitutes the first line of defense against inhaled particles containing aeroallergens that triggers a pro-inflammatory innate immune response, at the level of bronchioles we can find Clara cells with microvilli, without cilia, in her cytoplasm there are secretion granules, which reflects its function as a steam secretory cell, its number increases with decreasing hair cells and constitutes 22% of the cell mass in the bronchioles [8, 21].

Normally, the lungs when exposed to irritating, allergic or infectious stimuli, respond with a significant increase in mucin-producing cells in both mice and humans, which is dependent on IL-13 signaling. This increased mucosal response generates a differentiated cell that can no longer enter the cell cycle, which provides critical protection to the respiratory tract but leads to loss of repair potential [21].

Gandhi and Vliagoftis [8] has described the effect of allergens on the epithelium by irritating them with the consequent mucous secretion, increased permeability of the epithelia, which facilitates the entry of allergens and their capture by dendritic cells that leads to Dendritic cell interactions towards the activation of Th2 cells, that are part of type 1 hypersensitivity, is characterized by the secretion of cytokines that signal eosinophils, basophils, mast cells and lymphocytes, which produce the effector cytokines that characterize the allergic response such as IL4, IL-5 and IL-13 and pro-

duction of IgE [17]. In humans, the relationship of IgE production from birth and its relationship with IL-4, IL-13, IL-4 is essential for the differentiation of lymphocytes to CD4⁺ producers of IL-13 that leads to airway hyperreactivity, mucus production and subepithelial fibrosis [17]. IL-4 and IL-13 share a receptor complex: (IL4R α / IL-13R α 1) and work to promote the isotype change to IgE of B lymphocytes. When IgE binds to its receptor in mast cells and basophils, cellular activation and degranulation occurs with the recruitment of other inflammatory cells in the airways [17]. Another type 2 cytokine is IL-5, which is critical for the proliferation, maturation and chemotaxis of eosinophils, that release the cationic protein content in their granules, the neurotoxin derived from eosinophils, and the main basic protein that causes local inflammation in airway tissue [5].

The mechanisms described above coincide with our results, that is, we detect a pattern of cells that produce and secrete IL-4, IL-5, IL-13 that regulate the production of systemic IgE that is characteristic of the allergic type inflammatory response, as well as inflammatory modifications in the lung tissue, we also corroborate it with the detection of the expression of the IL-4 mRNA in tissues, so we can say that cypermethrin induces both local and systemic allergic inflammation when administered by inhalation.

6. Conclusions

In Wistar rat exposed to cypermethrin in a model of chronic poisoning via inhalation:

1. There were clinical signs of hypersensitivity with greater severity between 7 and 14 days of treatment.
2. There was an inflammatory response in the lung characterized by the expression of IL-4, IL-5 and IL-13 and an increase in eosinophils recruited according to the exposure time.
3. A 5-fold increase in serum IgE concentration was detected after 14 days of treatment with respect to the control.

7. Funding Details

This work was supported by CONACYT Mexico, under grant to Cristina González Ramírez number 471950.

References

1. Erin LA, Weston DP, Ureda NM. Use and Toxicity of Pyrethroid Pesticides in the Central Valley, California, USA. *Environmental Toxicology and Chemistry*. 2005; 24 (4): 966-72.
2. Benítez-Bribiesca L, Pérez-Astudillo L, Freyre-Horta R. Histological Stain for Major Basic Protein in Eosinophil Granulocytes and Spermatozoa with Alkaline Erythrosin B. *Archivos De Investigacion Medica*. 1987; 18(3): 213-8.
3. Choi H, Moon JK, Liu KH, Park HW, Ihm YB, Park BS, Kim JH. Risk Assessment of Human Exposure to Cypermethrin during Treatment of Mandarin Fields. *Archives of Environmental Contamination and Toxicology*. 2006; 50 (3): 437-42.
4. Jonathan C, Bonvalot Y, Carrier G, Lapointe C, Fuhr U, Tomalik-Scharte D, et al. A Novel Toxicokinetic Modeling of Cypermethrin and Permethrin and Their Metabolites in Humans for Dose Reconstruction from Biomarker Data. *Plos One*. 2014; 9(2): e88517.
5. Elena C, Lohman IC, Guerra S, Wright AL, Halonen M. Association of IL-5 Cytokine Production and in Vivo IgE Levels in Infants and Parents. *Journal of Allergy and Clinical Immunology*. 2007; 120(4): 820-6.
6. Cruse G, Kaur D, Yang W, Duffy SM, Brightling CE, Bradding P. Activation of Human Lung Mast Cells by Monomeric Immunoglobulin E. *European Respiratory Journal*. 2005; 25(5): 858-63.
7. Ana FT, Clarà PC. Deposition of Inhaled Particles in the Lungs. *Archivos De Bronconeumologia*. 2012; 48(7): 240-6.
8. Vivek DG, Vliagoftis H. Airway Epithelium Interactions with Aeroallergens: Role of Secreted Cytokines and Chemokines in Innate Immunity. *Frontiers in Immunology*. 6. 2015.
9. Azucena CGA, Robledo-Marengo ML, Medina- Díaz IM, Velázquez-Fernández JB, Girón-Pérez MI, Quintanilla-Vega B, et al. Patrón De Uso Y Venta De Plaguicidas En Nayarit, México. 2010; 8.
10. Hénault-Ethier L. Health and Environmental Impacts of Pyrethroid Insecticides: What We Know, What We Don't Know and What We Should Do about It - Executive Summary and Scientific Literature Review. 2016.
11. Hideo K. Pyrethroids: Mammalian Metabolism and Toxicity. *Journal of Agricultural and Food Chemistry*. 2011; 59 (7): 2786-91.
12. James EL. Five Office Workers Inadvertently Exposed to Cypermethrin. *Journal of Toxicology and Environmental Health*. 1992; 35(4): 261-7.
13. Xiu-Min L, Serebrisky D, Lee SY, Huang CK, Bardina L, Schofield BH, et al. A Murine Model of Peanut Anaphylaxis: T- and B-Cell Responses to a Major Peanut Allergen Mimic Human Responses. *Journal of Allergy and Clinical Immunology*. 2000; 106(1): 150-8.
14. Paula LL, Kim LK, Palm NW, Flavell RA. TH2, Allergy and Group 2 Innate Lymphoid Cells. *Nature Immunology*. 2013; 14(6): 536-42.
15. Laurie AM, Wechsler ME. Selecting the Right Biologic for Your Patients with Severe Asthma. *Annals of Allergy, Asthma & Immunology*. 2018; 121(4): 406-13.
16. Marsha KM, MacMillan DK, Zehr D, Sobus JR. Pyrethroid Insecticides and Their Environmental Degradates in Repeated Duplicate-Diet Solid Food Samples of 50 Adults. *Journal of Exposure Science & Environmental Epidemiology*. 2018; 28(1): 40-5.
17. Toshinori N, Hirahara K, Onodera A, Endo Y, Hosokawa H, Shinoda K, et al. Th2 Cells in Health and Disease. *Annual Review of Immunology*. 2017; 35(1): 53-84.
18. Lucette P, Savignac M. Involvement of Ion Channels in Allergy. *Current Opinion in Immunology*. 2018; 52: 60-7.

19. Edna PB, Armed Forces Institute of Pathology (U.S.). Laboratory Methods in Histotechnology. Washington, D.C.: American Registry of Pathology. 1992.
20. Susan DR, Malkinson AM. Clara Cell: Progenitor for the Bronchiolar Epithelium." *The International Journal of Biochemistry & Cell Biology*. 2010; 42(1): 1-4.
21. Sánchez-Alemán E, Quintanar-Stephano A, Escobedo G, Campos-Esparza MR, Campos-Rodríguez R, Ventura-Juárez J. Vagotomy Induces Deregulation of the Inflammatory Response during the Development of Amoebic Liver Abscess in Hamsters. *Neuroimmunomodulation*. 2015; 22(3): 166-80.
22. Zane V, Pilmane M. Inflammatory, Anti-Inflammatory and Regulatory Cytokines in Relatively Healthy Lung Tissue as an Essential Part of the Local Immune System. *Biomedical Papers*. 2017; 161(2): 164-73.
23. Brian AW. Inhalation Exposure Systems: Design, Methods, and Operation: *Toxicologic Pathology*. 2007; 35(1): 3-14.
24. Yamada Y, Yoshihara S, Arisaka O. Creola Bodies in Wheezing Infants Predict the Development of Asthma. *Pediatric Allergy and Immunology*. 2004; 15(2): 159-62.